# X-ray absorption in $Ce(Fe_{1-x}Co_x)_2$ and $Ce(Fe_{1-x}Al_x)_2$ compounds

Jesús Chaboy, Cristina Piquer, Luis M. García, and Fernando Bartolomé
*Instituto de Ciencia de Materiales de Aragón and Departamento de Física de la Materia Condensada, CSIC–Universidad de Zaragoza, 50009 Zaragoza, Spain*

Hirofumi Wada
*Department of Materials Science and Engineering, Kyoto University, Sakyo-ku, Kyoto 606-8501, Japan*

Hiroshi Maruyama and Naomi Kawamura
*Department of Physics, Faculty of Science, Okayama University, Okayama, Japan*
(Received 2 December 1999; revised manuscript received 10 February 2000)

We present in this work an x-ray absorption spectroscopy investigation performed at the $L_{1,3}$ edges of Ce and at the $K$ edge of iron and cobalt in the intermetallic compounds $Ce(Fe_{1-x}Co_x)_2$ and $Ce(Fe_{1-x}Al_x)_2$. The mixed-valence behavior of Ce is found to be preserved in both series upon Fe substitution. This result rules out the development of a localized $4f$ magnetic moment at Ce atoms driven by Fe-Co and Fe-Al substitution at the origin of the anomalous magnetic behavior of these series. A further confirmation has been obtained from the analysis of the x-ray magnetic circular dichroism spectra recorded at the Ce $L_{2,3}$ absorption edges.

## I. INTRODUCTION

In the past years a substantial amount of research has been done on $RCo_2$-$RFe_2$ systems to study the ways in which magnetic order sets in. Indeed, an innermost feature of the $RCo_2$ compounds, where $R$ is not magnetic, is that unlike the corresponding $RFe_2$ compounds, they never show magnetic order. Special interest has been focused on the magnetic properties of the $Ce(Fe_{1-x}Co_x)_2$ series ranging from the superconductivity of $CeCo_2$ to the reduced magnetic moment and low Curie temperature of $CeFe_2$.

$CeFe_2$ is a simple ferromagnet with a Curie temperature $T_c \simeq 230$ K.[1,2] Its magnetization behavior and the magnetic hyperfine field follow approximately the molecular-field theory with a $J=1/2$ Brillouin function.[2–5] The low value of the magnetic hyperfine field has been associated with both the reduced magnetic moment of the iron ions, $1.2\,\mu_B$, as compared to $1.7\,\mu_B$ in other $RFe_2$ compounds, and to the low $T_c$, which ranges between 500 and 700 K in other $RFe_2$ compounds.[6–10] The peculiar behavior of $CeFe_2$ within the $RFe_2$ series is also evidenced by the marked change of its magnetic properties upon hydrogen uptake: the saturation magnetization is about 70% higher than in the pure compound and $T_c$ increases up to 358 K. On the contrary, the decrease of $T_c$ and a slight increase of the Fe magnetic moment (25% for $YFe_2H_4$) are observed for the rest of the $RFe_2$ series.[11,12] Due to the reduced lattice parameter of $CeFe_2$, these anomalies were early ascribed to the transfer of the Ce $4f$ electron to the conduction band.[2] On these bases Ce was considered as tetravalent (nonmagnetic) in $CeFe_2$ while its electronic state changes to trivalent (magnetic) upon hydrogen uptake.[13,14]

However, the behavior of $CeFe_2$ upon Fe substitution has stimulated new studies on the instability of ferromagnetism in this compound. Substitution of Fe by a small amount of impurity destabilizes the ferromagnetism in $CeFe_2$, yielding to the total loss of ferromagnetism for $\sim 5\%$ Al substitution.[15,16] $Ce(Fe_{1-x}M_x)_2$ pseudobinaries with $M=(Co,Ru,Si,Os,Ir)$ exhibit similar magnetic instabilities,[17–21] whereas no instability is associated with the $M=(Ni,Cu,Rh,Mn)$ substitution.[21] Moreover, substitution of Y and U onto the Ce sites in these anomalous pseudobinaries results in a return to normal magnetic behavior.[16,22] All these results question the naive picture of nonmagnetic Ce in $CeFe_2$, pointing out the role of the hybridization between the $4f$- and $3d$-band electrons into determining the peculiar magnetic behavior of $CeFe_2$ and its related pseudobinaries compounds.[23,24]

The current model for the understanding of the $CeFe_2$ magnetic properties upon Fe substitution considers both that its ferromagnetism is very close to some type of instability and that the itinerancy of the Ce $4f$ electrons could prevent the formation of $4f$ magnetic moments. Within this scenario one of the most striking features of the $Ce(Fe_{1-x}Co_x)_2$ series is the behavior of the Curie temperature ($T_c$) as a function of the Co content ($x$) that does not exhibit the expected linear decreasing.[20,25] These experimental findings pose the question regarding if the peculiar magnetic behavior of $CeFe_2$ under iron substitution is linked to the instability of cerium electronic state, to the peculiarity of the $4f$-$3d$ hybridization, or to the interplay of both effects.

In the light of the peculiar magnetic properties of $Ce(Fe_{1-x}Co_x)_2$ it would be particularly interesting to see how the Ce valence and the $4f$-$5d$-$3d$ hybridization behave between $CeFe_2$ and $CeCo_2$. With this aim in mind we have performed a systematic x-ray absorption spectroscopy (XAS) and x-ray magnetic circular dichroism (XMCD) study at the $L_{1,2,3}$ edges of Ce and at the Fe and Co K edges. Our results indicate that the Ce valence does not vary through the solid solution while Co induces strong electronic changes that are at the origin of the anomalous magnetic behavior of this series. In order to get further confirmation of this last point,

 

we have also extended our study to the case of the $Ce(Fe_{1-x}Al_x)_2$ series.

## II. EXPERIMENT

$Ce(Fe_{1-x}Co_x)_2$ samples with $x=$ (0, 0.1, 0.2, 0.3, 0.4, 0.5, 0.6, 0.8, and 1) and $Ce(Fe_{1-x}Al_x)_2$ samples with $x=$(0.01, 0.035, and 0.05) were prepared by argon arc-melting of pure constituents of at least nominal 99.9% purity, followed by annealing at 850 °C in a evacuated quartz tube for 1 week. Both phase and structural analyses were performed by using a standard x-ray diffractometer. *X*-ray analyses have shown that all the samples present a single-phase *C*15 Laves structure and that the lattice parameter of the pseudobinary compounds obeys Vegard's law, in agreement with previous reports.[25,26]

The magnetic measurements were performed by using a commercial superconducting quantum interference device (SQUID) magnetometer (Quantum Design MPMS-S5) equipped with an ac susceptibility attachment. XAS experiments were carried out at the ESRF BM29 XAFS beamline. The storage ring was operated in 2/3 filling mode with typical currents between 150 and 200 mA at an electron beam energy of 6 GeV. XAS experiments were performed in the transmission mode on homogeneous thin layers of the powdered samples at both Fe and Co *K* edges and at the Ce $L_{1,3}$ edges. Both magnetization and absorption experiments were carried out on the same polycrystalline samples. The fixed-exit double-crystal monochromator was equipped with a pair of Si (111) crystals with energy resolution $\Delta E/E \sim 2\times10^{-4}$. Silicon photodiodes were used to detect the incident and transmitted flux providing a full linear energy response.[27]

The absorption spectra were analyzed according to standard procedures: the background contribution from previous edges $\mu_B(E)$ was fitted with a linear function and subtracted from the experimental spectrum $\mu(E)$. Then, spectra were normalized to the absorption coefficient at $\sim$100 eV above the edge to eliminate thickness dependence.

XMCD measurements at the Ce $L_{2,3}$ edges were carried out at the beamline 28B of the Photon Factory (PF) synchrotron radiation facility of the National Laboratory for High Energy Physics (KEK) in Tsukuba. The PF storage ring was operated with a positron beam energy of 2.5 GeV and a maximum stored current of 360 mA. The x-ray radiation was monochromatized by using a Si(111) double-crystal monochromator, the degree of circular polarization after monochromatization being $P_c \sim 0.3$.[28] The XMCD measurements were performed in the transmission mode, on the same powder layers as for the XAS experiments, at different fixed temperatures from 300 K to 50 K for several $Ce(Fe_{1-x}Co_x)_2$ samples by using a closed-cycle He cryostat. The XMCD spectra were recorded by reversing the sample magnetization for a fixed polarization of the incoming radiation. In our experimental setup a magnetic field of 1 T was applied parallel to the plane of the sample at 45° to the incident beam and reversed twice for each energy value.

The spin-dependent absorption coefficient was then obtained as the difference of the absorption coefficient $\mu_c=(\mu^- - \mu^+)$ for antiparallel, $\mu^-$, and parallel, $\mu^+$, orientation of the photon helicity and sample magnetization. As in the case of the XAS measurements, XMCD spectra were normalized to the averaged absorption coefficient at high energy to eliminate thickness dependence.

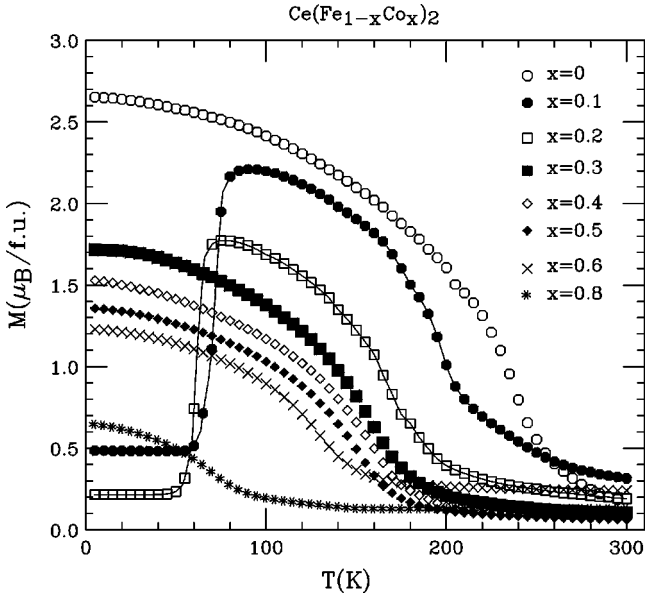


FIG. 1. Temperature dependence of magnetization for the $Ce(Fe_{1-x}Co_x)_2$ series measured under an external applied field of 10 kOe.

## III. RESULTS AND DISCUSSION

The magnetization of the investigated $Ce(Fe_{1-x}Co_x)_2$ samples measured under an applied field of 10 kOe is shown in Fig. 1. The magnetization ($M$) vs temperature ($T$) behavior of $CeFe_2$ shows a transition from the high-temperature paramagnetic phase (PM) to the ferromagnetic one (FM) taking place at about 236 K. The temperature at which the PM-FM transition occurs diminishes as increasing Co content to be $T_c \simeq 69$ K for $x=0.8$. In the case of $CeCo_2$ the ferromagnetic character is lost through the entire temperature range investigated (from room temperature to 4.2 K).

In the case of $Ce(Fe_{0.9}Co_{0.1})_2$ and $Ce(Fe_{0.8}Co_{0.2})_2$ the substitution of Fe by Co results in the appearance of a second transition at a temperature $T_S=72$ K and 62 K, respectively. At this second transition the ferromagnetism evolves into a canted spin structure, with a decreasing of the ferromagnetic moment which is completely lost as more Fe is replaced.[18,19,29,30]

Another peculiar feature in the magnetic behavior of the $Ce(Fe_{1-x}Co_x)_2$ series is the dependence of the Curie temperature with the cobalt content. As shown in Fig. 2, while the lattice parameter shows a linear decrease as cobalt content ($x$) increases, $T_c$ departs from a linear behavior between $x=0.2$ and 0.7, showing a relative minimum for $x=0.3$ and a relative maximum at $x=0.4$.

### A. XAS study on $Ce(Fe_{1-x}Co_x)_2$ and $Ce(Fe_{1-x}Al_x)_2$ series

Because the complexity of the magnetic phase diagram has been often related to the special character of Ce in $CeFe_2$, it is needed to determine if the Ce valence changes upon Fe substitution.

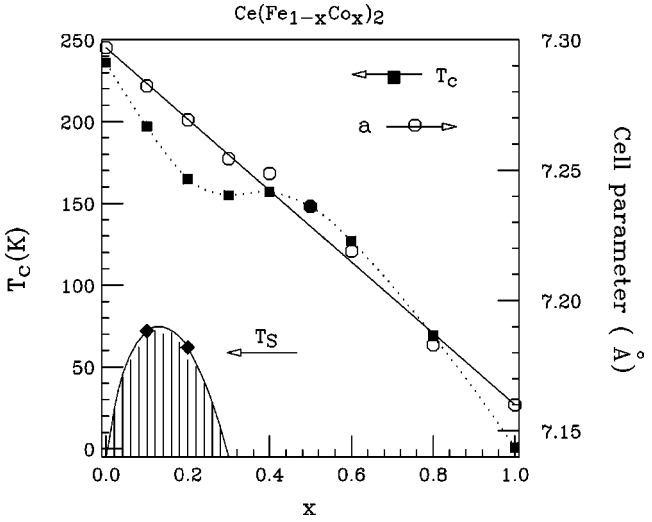


FIG. 2. Comparison between magnetic ordering temperature, $T_c$ (■) and lattice parameter (○) behavior as a function of the cobalt content in the $Ce(Fe_{1-x}Co_x)_2$ series. For the sake of completeness the temperature of the second magnetic transition from ferromagnetic to canted spin structure, $T_S$ (◇), is also shown.

To this end we have recorded the XAS spectra at the Ce $L_3$ edge through the whole $Ce(Fe_{1-x}Co_x)_2$ series. The results, compiled in Fig. 3, show that for all the investigated compounds the Ce $L_3$-edge absorption exhibits a double-peak profile at the edge, characteristic of a mixed-valence character.[31] Moreover, no significant changes are found in the intensity, width, and relative energy position of the two white lines. Our results indicate that the Ce mixed-valence behavior is retained in all the $Ce(Fe,Co)_2$ systems, the Ce valence being about 3.3.

The immediate conclusion that one can obtain from this Ce $L_3$ absorption analysis is that the peculiar $T_c$ vs cobalt content behavior is not due to the modification of the cerium electronic state upon Fe substitution. To get a deeper insight into the origin of this behavior and to try to individuate if the addressed ferromagnetic instability is due to some specific

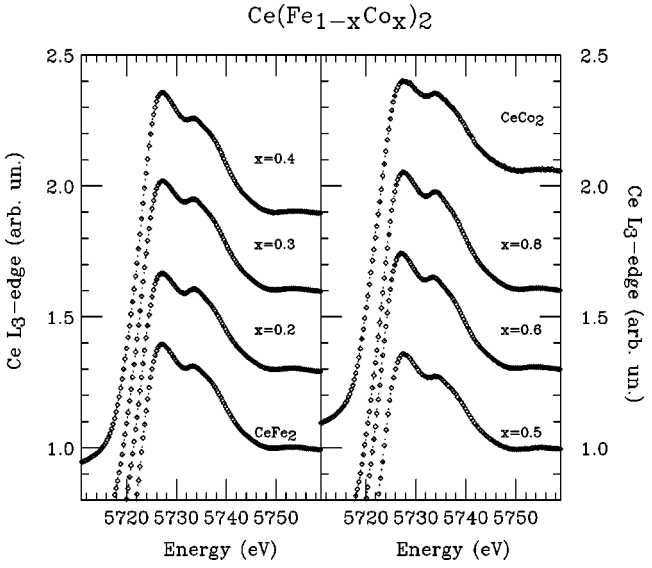


FIG. 3. Comparison between the experimental XAS spectra at the Ce $L_3$ edge in the case of $Ce(Fe_{1-x}Co_x)_2$ compounds.

element of the alloy (Ce, Fe, or Co), we have extended our analysis to further absorption edges. The main reason is to take advantage of the site and atom selectivity offered by x-ray absorption, in such a way that by tuning the photon energy near Fe, Co, and Ce absorption edges, we can probe both the local geometry and the electronic state of the selected atomic specie.

We have recorded XAS spectra experiments at both Fe and Co $K$ edges and at the Ce $L_1$ edge in the $Ce(Fe_{1-x}Co_x)_2$ series. At both absorption edges one electron is excited from an inner $s$ level and promoted to a final $p$-symmetry state. Thus the edge spectrum probes the unoccupied local and partial $p$ density of states projected on the absorbing atom. What is noticeable is that the spectral shape of the $L_1$ spectra in all the lanthanide metals exhibits a steplike rise of the absorption at the threshold that is absent in the case of rare-earth vapors.[32] The explanation for such behavior is that in the vapors the atomic resonances corresponding to the one-electron transition $s \rightarrow p$ are very weak,[33,34] while upon condensation into the metallic state, the outer $p$-symmetry orbitals are strongly hybridized with the outer $s$- and $d$-symmetry orbitals. Consequently, the shoulderlike feature at the edge reflects the high density of empty $5d$ states via hybridization of the $sp$ and $5d$ empty states, the modification of the width and intensity of this spectral feature being a fingerprint of the hybridization changes.[35,36]

Figure 4(a) shows the comparison of the Ce $L_1$-edge absorption in both $CeFe_2$ and $CeCo_2$ and several intermediate concentrations. What is observed is the progressive enhancement of the shoulderlike feature as the cobalt content increases, indicating a higher hybridization between the conduction states of cerium and those of Fe and Co. This result can be understood as due to the contraction of the crystal cell as the Co content increases. This contraction implies a widening of the $d$ bands and consequently the increase of the (Fe,Co) $3d$ and Ce $5d$ overlap, as experimentally observed.

The effect at the edge is found to be gradual, as the evolution of the crystal-cell parameter, so that it seems reasonable to think that neither changes of the Ce electronic state nor Ce($5d$) hybridization play a crucial role in driving the anomalous $T_c$ behavior, the effect being more likely due to the effect of the transition metal in the density of states (DOS). Indeed, the complex magnetic behavior of Laves-phase compounds with Mn, Fe, Co, and Ni has been accounted for according to the peculiar shape of the DOS.[37,38] The shape of the DOS calculated by different methods is characterized by the existence of two sharp peaks, mainly of $M$ $3d$ states, near the Fermi level $E_F$. Early calculations of the electronic structure of $CeCo_2$ have shown a strong $3d$-$4f$ hybridization, so that the weight of the Ce $5d$ component in the density of states at the Fermi energy is very small while that of the $4f$ component is very large, resulting in a high density of states at the Fermi level.[39] This result is in agreement with the suggestion of Rastogi *et al.* to account for the large electronic specific heat coefficient of $CeCo_2$,[40] and it is supported by more recent band calculations.[24,41] The new calculations showed not only the delocalized nature of the Ce $4f$ states in $CeFe_2$, but also that the $4f$-$3d$ hybridization decreases as the number of $3d$ electrons increases when going from $CeFe_2$ to $CeNi_2$, resulting in the narrowing of the $4f$ states. While for $CeFe_2$ the calculated DOS is rather large

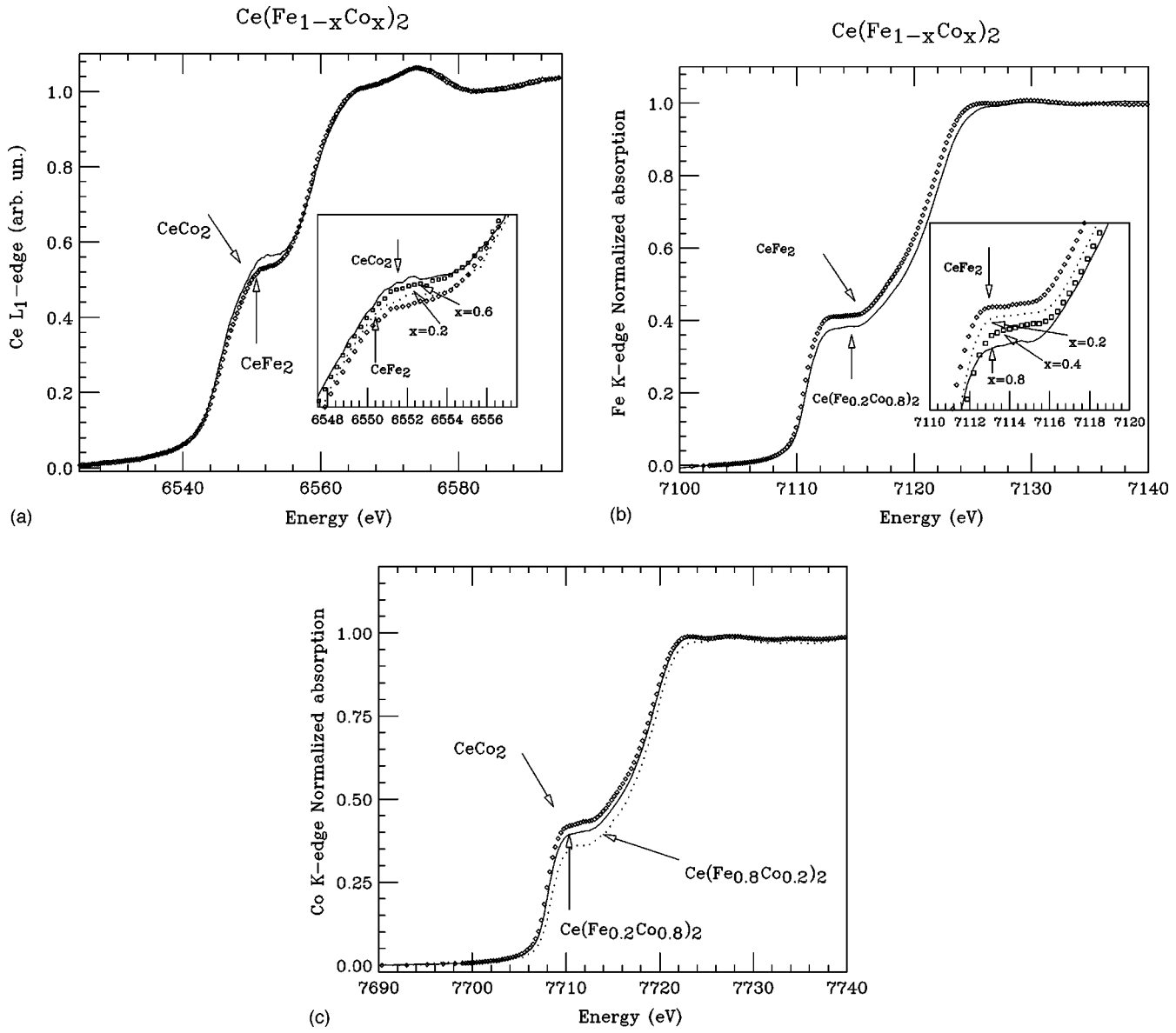


FIG. 4. Selected x-ray absorption spectra recorded in the $Ce(Fe_{1-x}Co_x)_2$ series at the (a) Ce $L_1$ edge, (b) Fe $K$ edge, and (c) Co $K$ edge.

at the Fermi level and the Stoner criterion for ferromagnetism is fulfilled, for $CeCo_2$ the Fermi level lies in a low DOS region so that the Stoner criterion is not fulfilled. The main conclusions derived from the calculations are (i) the fact that $CeFe_2$ satisfies Stoner criterion implies a ferromagnetic instability; (ii) the $3d$ states are responsible for the large DOS at $E_F$ in $CeFe_2$, and thus the iron states drive the magnetic instability and not the cerium $4f$ electrons; and (iii) the Fe($3d$)-Ce($4f$) hybridization is higher in $CeFe_2$ than in $CeCo_2$.

However, as pointed out by Fernández and co-workers, as Co substitution reduces the crystal-cell volume, it is expected that the hybridization of the Ce $4f$ orbital increases with the cobalt content while the Ce magnetic moment decreases, contrary to the Al substitution case in which the crystal cell is expanded.[42] The question arising is how important is the $3d$-$4f$ hybridization in determining the anomalous magnetic behavior of the $Ce(Fe_{1-x}Co_x)_2$ series. Indeed, the conclusion of a photoemission study of several $RCo_2$ systems including Ce, indicates that the hybridization between the $R$ $4f$ and Co $3d$ electrons is not that important in determining the Co $3d$ electronic structures in these systems.[43]

To have an insight into the influence of Fe-Co substitution into the DOS of the $Ce(Fe_{1-x}Co_x)_2$ series we present in Fig. 4(b) and Fig. 4(c) a comparison of the Fe and Co $K$-edge x-ray absorption for different Co concentrations, respectively. As the cobalt content increases, the intensity of the shoulderlike feature at the Fe $K$-edge absorption threshold clearly diminishes as compared to that of pure $CeFe_2$. Moreover, within the experimental resolution it is observed that the effect proceeds gradually as a function of $x$. These results evidence the existence of a strong electronic perturbation on the DOS driven by cobalt substitution. The decrease of the intensity of the shoulderlike resonance at the raising edge indicates that the local density of $p(d)$ states projected on the Fe sites is strongly reduced after the substitution. Moreover, it should be noted that while the observed effect—i.e., the electronic modification impact—is really large at the Fe sites [Fig. 4(a)], it is less marked at the Ce ones [Fig. 4(a)], in agreement with the $3d$ states being the dominant part of

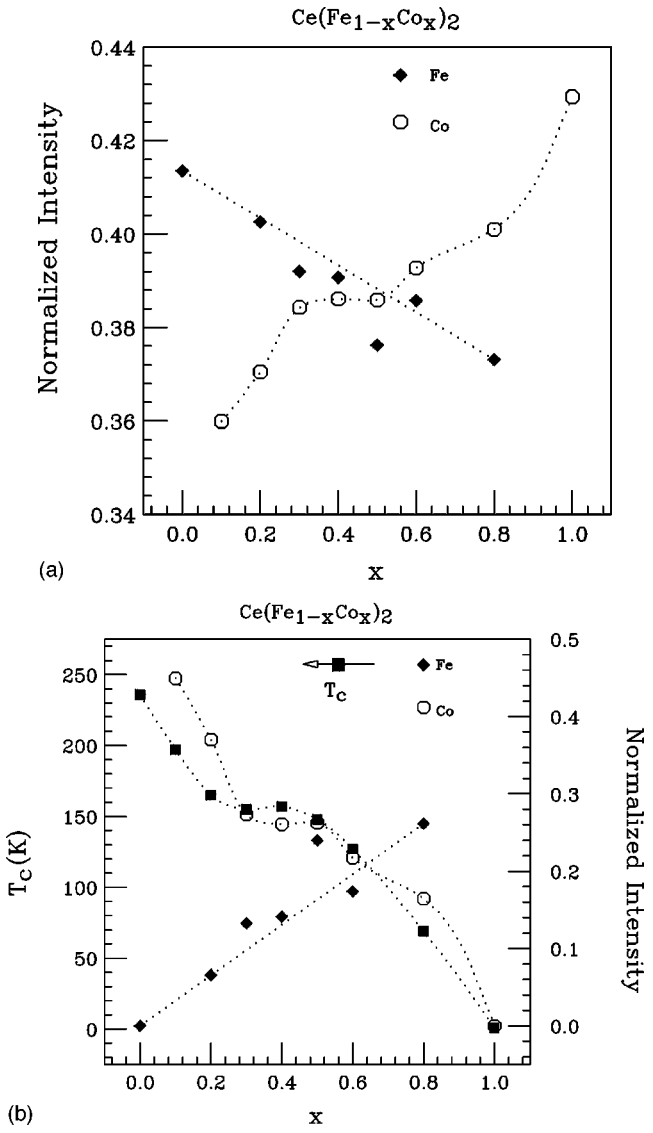


FIG. 5. (a) Comparison between the Co-content dependence of the absorption peak at the Fe ( $\diamond$ ) and Co $K$ edges ($\bigcirc$). (b) Comparison between the Co-content dependence of $T_c$ ($\blacksquare$) in the $Ce(Fe_{1-x}Co_x)_2$ series and that of $1/N_E$ for Fe ( $\diamond$ ) and Co ($\bigcirc$) (see text for details).

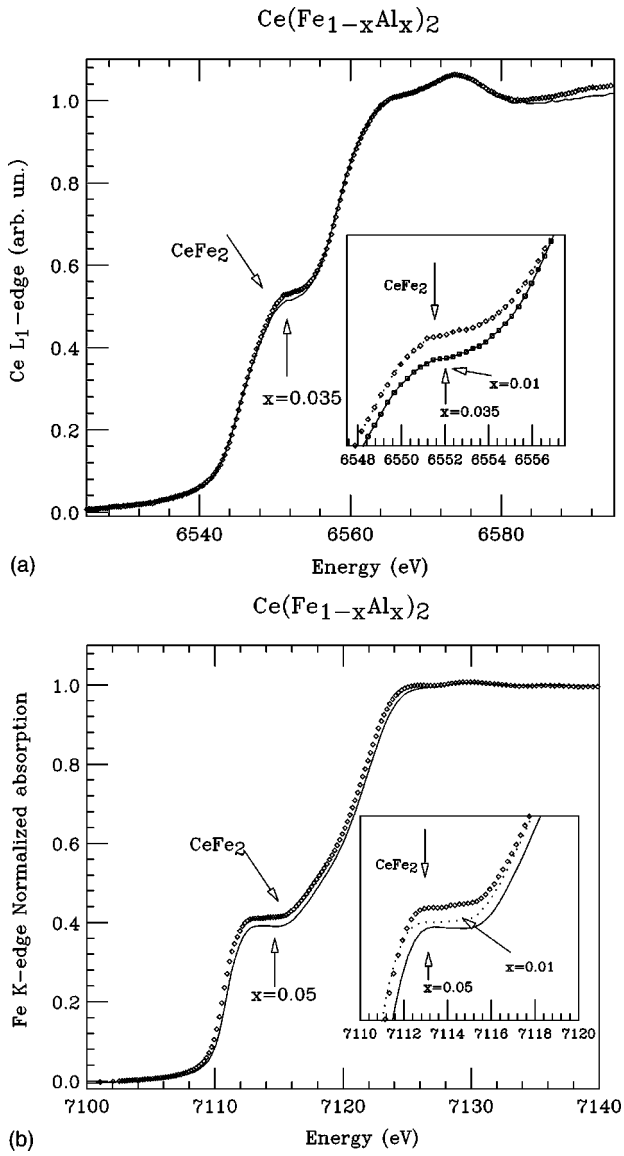


FIG. 6. Selected x-ray absorption spectra recorded in the $Ce(Fe_{1-x}Al_x)_2$ series at the Ce $L_1$ edge (a) and at the Fe $K$ edge (b).

the DOS at the Fermi level. According to the DOS calculations, the observed variation of the x-ray appearance near-edge structure (XANES) profile reported in Fig. 4(b) can be interpreted in terms of the progressive filling of the $d$ band of Fe (strongly hybridized to the empty $p$ states) as Co carries more $d$ electron to the system. In such a case and also because of the cell contraction and the subsequent band widening, the Fermi level lies in a area with a lower DOS. Thus, the ferromagnetic character is less favored as expected according to the Stoner criterion. This result and its interpretation in terms of DOS modification are supported for the observed behavior of the Co $K$-edge absorption through the whole $Ce(Fe_{1-x}Co_x)_2$ series shown in Fig. 4(c). The intensity of the absorption peak at the edge increases proceeding from $CeFe_2$ to $CeCo_2$ as the contribution of Co states to the DOS becomes dominant. Our results indicate that the effect of cobalt substitution on the DOS at the Fermi level of the system is the driving mechanism to explain the anomalous magnetic behavior. Study of Ce $L_1$-edge absorption suggests that, contrary to previous suggestions, the $3d$-$5d$-$4f$ hybridization is higher for $CeCo_2$ than in $CeFe_2$, in agreement with that expected from the reduction of the crystal-cell volume[42] and previous x-ray photoelectron spectroscopy (XPS) results.[43]

At this point it is instructive to compare the Co-content dependence of $T_c$ in the $Ce(Fe_{1-x}Co_x)_2$ series and the intensity of the absorption peak at the Fe and Co $K$ edge shown in Fig. 5. The local density of empty $p(d)$ states, $N_E$, projected on the Fe sites is progressively reduced after the substitution, in agreement with the expected filling of the $d$ band of Fe. On the contrary, the $N_E$ projected onto the Co sites shows a sharp increase going from low Co content towards $CeCo_2$. This result is in agreement with the pronounced localization of the Co $3d$ wave function on the atomic site.[43,44] This increase is not linear as in the Fe case but shows a plateau-like region between $x=0.3$ and 0.6, i.e., in the region of cobalt concentration in which $T_c$ in the $Ce(Fe_{1-x}Co_x)_2$ series departs from the linear behavior observed for the lattice

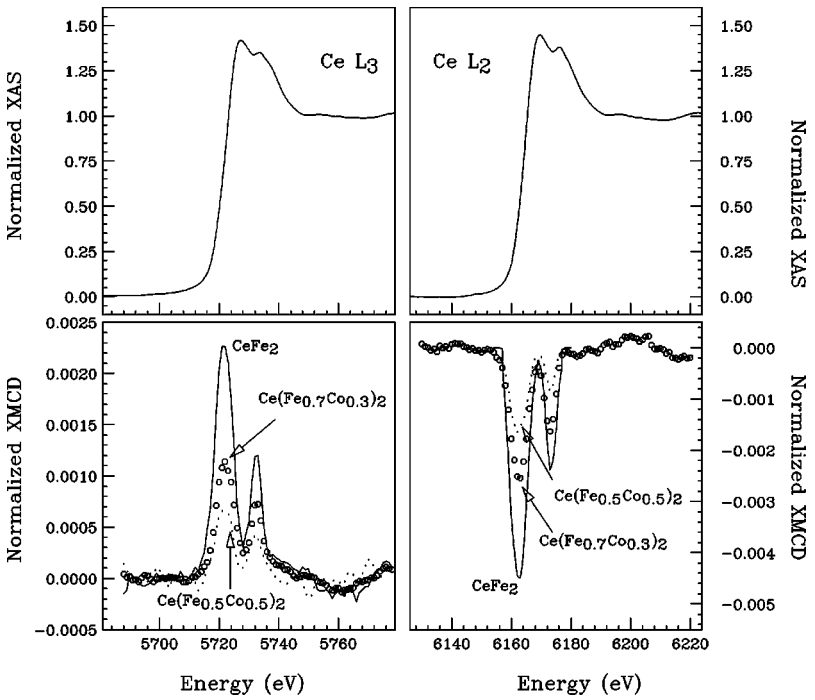


FIG. 7. Normalized Ce $L_{2,3}$ XMCD spectra of $CeFe_2$ (solid line), $Ce(Fe_{0.7}Co_{0.3})_2$ (○) and $Ce(Fe_{0.5}Co_{0.5})_2$ (dotted line) recorded at $T = 140$ K: Ce $L_3$ edge (left panel), Ce $L_2$ edge (right panel). In the top panel the normalized XANES spectra of $Ce(Fe_{0.7}Co_{0.3})_2$ at the Ce $L_3$ (left) and Ce $L_2$ (right) edges are shown.

parameter. The relationship between the anomalous behavior of $T_c$ and cobalt $N_E$ is made more evident in Fig. 5(b), where $T_c$ and $1/N_E$ of Fe and Co are plotted as a function the cobalt content.

Further verification of these conclusions has been obtained by performing the same class of studies on the $Ce(Fe_{1-x}Al_x)_2$ series. In this series Al substitution leads to the loss of ferromagnetism but the crystal cell is expanded upon substitution contrary to the Fe-Co case. As in the case of the $Ce(Fe,Co)_2$ systems, Ce $L_3$ spectra show that the mixed-valence behavior is retained upon small Al substitution, the Ce valence being about 3.3 too, while in $CeAl_2$ the double-peak structure characteristic of mixed-valence behavior disappears and only the white line corresponding to the $4f^1$ configuration—i.e., magnetic Ce—is evidenced. Ce $L_1$-edge absorption, reported in Fig. 6(a), shows the decrease of the shoulderlike feature as the Al content increases, contrary to the case of cobalt substitution. This result indicates a lowering of the Ce($5d$)-(Fe,Co)($3d$) hybridization, as expected due to the expansion of the cell induced by Al substitution. On the other hand, when looking at the Fe $K$ edge, Fig. 6(b), a similar result is found to the case of the cobalt-substituted samples; i.e., the intensity of the feature at the threshold is depleted with respect to that of $CeFe_2$. In principle, this result seems to be in contradiction with the above discussion because the narrowing of the DOS due to Al substitution would result in a higher DOS at the Fermi level, thus reinforcing the structure at the Fe $K$ edge. However, it should be noted that despite the fact that Fe substitution by Al implies a volume expansion accompanied by the narrowing of the DOS and thus the Fermi level would lie in a higher DOS region, Al has no $3d$ states near the Fermi level so that the electronic structure is modified, resulting in a depletion of the DOS where the Fermi level lies.

### B. XMCD study of the $Ce(Fe_{1-x}Co_x)_2$ series

The picture emerging from the conclusions of the preceding section is that the magnetic state of cerium atoms does not change upon Fe substitution in both $Ce(Fe_{1-x}Co_x)_2$ and $Ce(Fe_{1-x}Al_x)_2$. Then it is expected that cerium exhibits a similar magnetic behavior to that of $CeFe_2$; i.e., no localized $4f$ magnetic moment is present in the system.

In order to get experimental confirmation of this point we have performed a systematic XMCD study at the Ce $L_{2,3}$ edges as a function of temperature and cobalt concentration in the $Ce(Fe_{1-x}Co_x)_2$ series.

The Ce $L_{2,3}$-edge XMCD signals for selected cobalt concentrations are shown in Fig. 7. In all the cases, the XMCD signal at the Ce $L$ edges in the $Ce(Fe_{1-x}Co_x)_2$ series exhibits a double-peak structure that resembles the existence of configurational mixing in the ground state, as in the case of polarization-averaged XAS spectra (see Fig. 3). What is found is that the intensity of the XMCD signals decreases as the cobalt content increases but the energy separation between the two peaks remains unaltered. This is direct confirmation that the cerium electronic state does not change through the whole series. Moreover, it is an indication that the magnetic moment induced on Ce sites is induced by the transition metal.

According to Brouder and Hikam[45] the XMCD signals, defined as above, at the $L_{2,3}$ edges are proportional to the reduced transition probability towards spins parallel (antiparallel) to the net magnetization of the sample, $\sigma^{\uparrow(\downarrow)}$, through the relations $\mu_c \alpha \sigma^{\uparrow} - \sigma^{\downarrow}$ and $\mu_c \alpha \sigma^{\downarrow} - \sigma^{\uparrow}$ for the $L_2$ and $L_3$ edges, respectively. The positive (negative) sign of the Ce XMCD signal at the $L_3$ ($L_2$) edge indicates that the Ce $5d$ spin is antiparallel with respect to the magnetization direction in the material. The magnetization in the material is governed by the transition metal, so that we are probing directly an antiparallel coupling between both Fe magnetic moment and that induced on the Ce sites of mainly $5d$ origin.

Despite there being a general consensus concerning that there is a net moment on the Ce site, mostly spin, and antiparallel to that of Fe, there is a hot debate regarding the value

TABLE I. Values of $\mu_{Ce_5d}$ for the $Ce(Fe_{1-x}Co_x)_2$ compounds derived from the XMCD spectra.

| $x$ | $T$(K) | $\langle L_z\rangle$ | $\langle S_z\rangle$ | $\langle L_z\rangle+2\langle S_z\rangle$ | $L_z/S_z$ |
|---|---|---|---|---|---|
| 0 | 130 | $-0.004\pm0.002$ | $-0.123\pm0.03$ | $-0.25\pm0.06$ | 0.036 |
| 0.3 | 140 | $-0.001\pm0.001$ | $-0.057\pm0.01$ | $-0.115\pm0.03$ | 0.017 |
| 0.3 | 130 | $-0.003\pm0.001$ | $-0.062\pm0.01$ | $-0.127\pm0.03$ | 0.048 |
| 0.3 | 100 | $-0.004\pm0.002$ | $-0.081\pm0.02$ | $-0.165\pm0.04$ | 0.049 |
| 0.3 | 80 | $-0.004\pm0.002$ | $-0.084\pm0.02$ | $-0.172\pm0.04$ | 0.048 |
| 0.3 | 50 | $-0.005\pm0.002$ | $-0.094\pm0.02$ | $-0.192\pm0.04$ | 0.053 |
| 0.4 | 140 | $-0.002\pm0.001$ | $-0.050\pm0.01$ | $-0.102\pm0.02$ | 0.040 |
| 0.4 | 100 | $-0.004\pm0.002$ | $-0.061\pm0.01$ | $-0.134\pm0.03$ | 0.065 |
| 0.5 | 130 | $-0.005\pm0.002$ | $-0.039\pm0.01$ | $-0.083\pm0.02$ | 0.130 |

of the moments (both $4f$ and $5d$).[46] Trying to obtain a deeper insight into the magnitude of $\mu_{Ce}(5d)$ in this series, we have applied the sum rules derived by Thole and coworkers to the XMCD spectra (corrected for the rate of circular polarization).[47] For the Ce $L_{2,3}$ edges they can be written as $\langle L_z\rangle=2(A_3+A_2)(n_{5d}/\sigma_{tot})$ and $\langle S_z\rangle=3/2(A_3-2A_2)(n_{5d}/\sigma_{tot})-7/2\langle T_z\rangle$. $A_3$ and $A_2$ are the integrals over the dichroic signal at the $L_2$ and $L_3$ edges, respectively, $n_{5d}$ is the number of holes in the Ce $5d$ band, and $\sigma_{tot}$ is the unpolarized $2p\rightarrow5d$ cross section. According to Ref. 48 we have considered $\langle T_z\rangle=0$. We have used two different ways to estimate $(n_{5d}/\sigma_{tot})$: (i) we have deduced experimentally $\sigma_{tot}$ as $3/2(\sigma^+ + \sigma^-)$ and fixed to 9 the number of $5d$ holes, and (ii) we have estimated $n_{5d}/\sigma_{tot}$ from the experimental Ce $L_{2,3}$ spectra by subtracting the Ce $L_1$ spectrum as proposed by Vogel *et al.*[49]

The obtained results are shown in Table I. Several findings should be stressed. First, the modification of the magnetic moment extracted by using $n_{5d}=1.5$ as proposed by other authors[48] is well suited within the error bar. Second, the magnitude of the $\mu_{Ce}$ of $5d$ origin we found in $CeFe_2$ at $T=130$ K reaches $-0.26\,\mu_B$, and its extrapolation at 4.2 K yields $-0.29\,\mu_B$, to be compared with the $-0.3\,\mu_B$ value derived from band calculations.[24] Third, the application of the first sum rule returns a small but nonzero orbital component for this $Ce(5d)$ moment and this orbital component increases as the Co content does. What it is more remarkable is that both orbital and spin moments are parallel, indicating that the Ce $5d$ magnetic moment is due to overlapping with the transition metal. This is shown even more clearly in Fig. 8, where the temperature dependence of the spontaneous magnetization in the $Ce(Fe_{1-x}Co_x)_2$ series and the Ce $5d$ magnetic moment deduced from the XMCD signal by applying the sum rules are compared. As we can see there is a remarkable agreement between the whole magnetization of the system and that of the derived $Ce(5d)$ magnetic moment, indicating that this last is induced by the iron one.

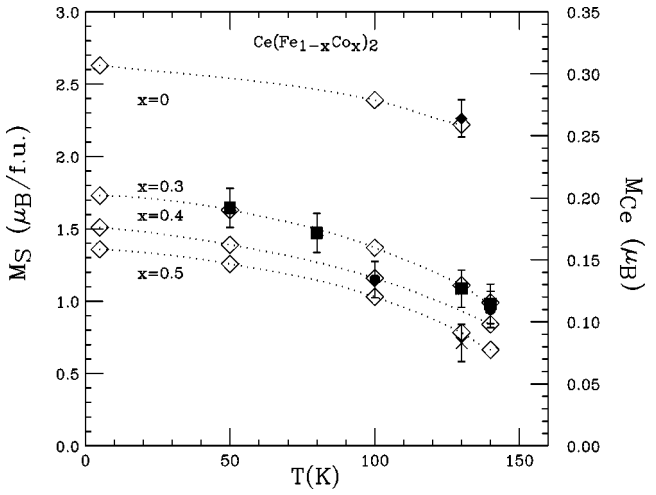


FIG. 8. Comparison of the temperature dependence of the spontaneous magnetization in the $Ce(Fe_{1-x}Co_x)_2$ series ( ◇ ) and the Ce $5d$ magnetic moment deduced from the XMCD signal by applying the sum rules.

## IV. SUMMARY AND CONCLUSIONS

In this work we have presented a detailed x-ray absorption spectroscopy and x-ray magnetic circular dichroism investigation performed at the $L$ edges of Ce and at the $K$ edge of iron and cobalt in the intermetallic compounds $Ce(Fe_{1-x}Co_x)_2$ and $Ce(Fe_{1-x}Al_x)_2$.

The analysis of the Ce $L_3$-edge absorption indicates that the mixed-valence behavior of Ce is preserved in both series upon Fe substitution. This result rules out the development of a localized $4f$ magnetic moment at Ce atoms driven by the Fe-Co and Fe-Al substitution at the origin of the anomalous magnetic behavior of these compounds. The combined analysis of the x-ray absorption spectra recorded at different edges in these systems indicates that the observed anomalous magnetic behavior is due neither to the cerium electronic state nor to the modification of the $4f$-$3d$ hybridization but it is determined by the influence of cobalt into the peculiar DOS of the system. The results of the present investigation are in agreement with electronic structure calculations, showing direct details of the reduction of the $f$-$d$ hybridization induced by Co substitution.

A further confirmation has been obtained from the analysis of the x-ray magnetic circular dichroism spectra recorded at the Ce $L_{2,3}$ absorption edges. Our results show the presence of a $Ce(5d)$ magnetic moment in the $Ce(Fe_{1-x}Co_x)_2$ series that is induced by the transition metal in agreement to previous experiments and theoretical calculations.

## ACKNOWLEDGMENTS

This work was partially supported by Spanish Grant Nos. DGICYT MAT96-0448 and MAT99-0667-C04-04. The experimental work at the European Synchrotron Radiation Facility has been performed with the approval of the European Synchrotron Radiation Facility (ESRF) Program Advisory Committee (Proposal HE-008). We are indebted to A. Filipponi for the technical support during the XAS measurements at the ESRF. We are also indebted to T. Iwazumi for the experimental support at KEK.

[1] J. Farrel and E. Wallace, J. Chem. Phys. **41**, 1924 (1964).
[2] K.H.J. Buschow and I.S. van Wieringen, Phys. Status Solidi **42**, 231 (1970).
[3] J. Farrel and E. Wallace, J. Chem. Phys. **41**, 1924 (1964).
[4] M. Rosen, H. Klimer, U. Atzmony, and M.P. Dariel, Phys. Rev. B **9**, 254 (1974).
[5] U. Atzmony and M.P. Dariel, Phys. Rev. B **10**, 2060 (1974).
[6] K.H.J. Buschow, Physica B **86-88**, 79 (1977).
[7] G.E. Fish, J.J. Rhyne, S.G. Sankar, and W.E. Wallace, J. Appl. Phys. **50**, 2053 (1979).
[8] C. Meyer, B. Srour, Y. Gros, and F. Hartman-Boutron, J. Phys. (Paris) **38**, 1449 (1977).
[9] J. Ilarraz and A. del Moral, Phys. Status Solidi A **57**, 89 (1980).
[10] C. Meyer, F. Hartman-Boutron, Y. Gros, Y. Berthier, and J.L. Buevoz, J. Phys. (Paris) **42**, 606 (1981).
[11] K.H.J. Buschow, Solid State Commun. **19**, 421 (1976).
[12] A.M. van Diepen and K.H.J. Buschow, Solid State Commun. **22**, 113 (1977).
[13] K.H.J. Buschow and A.M. van Diepen, Solid State Commun. **19**, 79 (1976).
[14] J. Chaboy, J. García, and A. Marcelli, J. Magn. Magn. Mater. **166**, 149 (1997).
[15] D.F. Franceschini and S.F. Da Cunha, J. Magn. Magn. Mater. **52**, 280 (1985).
[16] S.B. Roy and B.R. Coles, J. Phys.: Condens. Matter **1**, 419 (1989).
[17] S.B. Roy and B.R. Coles, J. Appl. Phys. **63**, 4094 (1988).
[18] S.J. Kennedy, A.P. Murani, B.R. Coles, and O. Moze, J. Phys. F: Met. Phys. **18**, 2499 (1988).
[19] S.J. Kennedy, A.P. Murani, J.K. Cockcroft, S.B. Roy, and B.R. Coles, J. Phys.: Condens. Matter **1**, 629 (1989).
[20] S.B. Roy and B.R. Coles, Phys. Rev. B **39**, 9360 (1989).
[21] S.J. Kennedy and B.R. Coles, J. Phys.: Condens. Matter **2**, 1213 (1990).
[22] S.B. Roy, G. Williams, and B.R. Coles, J. Phys. (Paris) **50**, 2733 (1989).
[23] P.K. Khowash, Phys. Rev. B **43**, 6170 (1991).
[24] O. Eriksson, L. Nordstrom, M.S.S. Brooks, and B. Johansson, Phys. Rev. Lett. **60**, 2523 (1988).
[25] H. Wada, M. Nishigori, and M. Shiga, J. Phys.: Condens. Matter **3**, 2083 (1991).
[26] G. Longworth and I.R. Harris, J. Less-Common Met. **41**, 175 (1975).
[27] J. Goulon, N.B. Brookes, C. Gauthier, J. Goedkoop, C. Goulon-Ginet, M. Hagelstein, and A. Rogalev, Physica B **208&209**, 199 (1995).
[28] T. Iwazumi, A. Koyama, and Y. Sakurai, Rev. Sci. Instrum. **66**, 1691 (1995); K. Hirano, T. Ishikawa, A. Koyama, and T. Iwazumi (unpublished).
[29] A.K. Rastogi and A.P. Murani, in *Theoretical and Experimental Aspects of Valence Fluctuations and Heavy Fermions*, edited by L.C. Gupta and S. K. Malik (Plenum, New York, 1987).
[30] R.G. Pillay, A.K. Grover, V. Balasubramanian, A.K. Rastogi, and P.N. Tandon, J. Phys. F: Met. Phys. **18**, L63 (1988).
[31] J. Röhler, J. Magn. Magn. Mater. **47&48**, 175 (1985).
[32] G. Materlik, B. Sonntag, and M. Tausch, Phys. Rev. Lett. **51**, 1300 (1983).
[33] G. Materlik, J.E. Müller, and J.W. Wilkins, Phys. Rev. Lett. **50**, 267 (1983).
[34] J.E. Müller and J.W. Wilkins, Phys. Rev. B **29**, 4331 (1984).
[35] A. Bianconi, in *X-ray Absorption: Principles, Applications, Techniques of EXAFS, SEXAFS and XANES*, edited by D.C. Koningsberger and R. Prins (Wiley, New York, 1988), Chap. 11, and references therein.
[36] J. Chaboy, A. Marcelli, and L. Bozukov, J. Phys.: Condens. Matter **7**, 8197 (1995).
[37] K. Terao and M. Shimizu, Phys. Lett. **95A**, 111 (1983); **104A**, 113 (1984).
[38] H. Yamada, J. Inoue, K. Terao, S. Kanda, and M. Shimizu, J. Phys. F: Met. Phys. **14**, 1943 (1984); H. Yamada, Physica B **149**, 390 (1988).
[39] A. Yanase, J. Phys. F: Met. Phys. **16**, 1501 (1986).
[40] A.K. Rastogi, G. Hilscher, E. Gratz, and N. Pillmayr, J. Phys. (Paris), Colloq. **49**, C8-277 (1988).
[41] L. Severin and B. Johansson, Phys. Rev. B **50**, 17 886 (1994).
[42] G.E. Fernández, M. Gómez Berisso, O. Trovarelli, and J.G. Sereni, J. Alloys Compd. **261**, 26 (1997).
[43] J.-S. Kang, J.H. Hong, J.I. Jeong, S.D. Choi, C.J. Yang, Y.P. Lee, C.G. Olson, B.I. Min, and J.W. Allen, Phys. Rev. B **46**, 15 689 (1992).
[44] L. Duo, P. Vavassori, L. Braicovich, and G.L. Olcese, Phys. Rev. B **51**, 4751 (1995).
[45] C. Brouder and M. Hikam, Phys. Rev. B **43**, 3809 (1991).
[46] A.P. Murani and P.J. Brown, Europhys. Lett. **48**, 353 (1999); A. Delobbe, A.-M. Dias, M. Finazzi, L. Stichauer, J.-P. Kappler, and G. Krill, *ibid.* **48**, 355 (1999).
[47] B.T. Thole, P. Carra, F. Sette, and G. van der Laan, Phys. Rev. Lett. **68**, 1943 (1992); P. Carra, B.T. Thole, M. Altarelli, and X. Wang, *ibid.* **70**, 694 (1993).
[48] A. Delobbe, A.-M. Dias, M. Finazzi, L. Stichauer, J.-P. Kappler, and G. Krill, Europhys. Lett. **43**, 320 (1998).
[49] J. Vogel, A. Fontaine, V. Cros, F. Petroff, J.P. Kappler, G. Krill, A. Rogalev, and J. Goulon, Phys. Rev. B **55**, 3663 (1997).